Bulletin of the Geological Survey of Japan, vol.57 (5/6), p. 143- 158 , 2006

REE resource evaluation of some alkaline granites and their weathered crust in South Korea

Shunso Ishihara[1], Kohei Sato[2], Yong-Joo Jwa[3] and Jong-Sun Kim[3]

Shunso Ishihara, Kohei Sato, Yong-Joo Jwa and Jong-Sun Kim (2006) REE resource evaluation of some alkaline granites and their weathered crust in South Korea. *Bull. Geol. Surv. Japan*, vol. 57 (5/6), 143-158, 14 figs, 5 tables, 2 appendix tables.

Abstract: A reconnaissance chemical study was made on four granitic bodies in South Korea, on which high REE contents are expected. Triassic foliated granite of the Daegang body occurring along the boundary between the Yeongnam-Ogcheon terrains contains average REE+Y content of 414 ppm and the L/HREE ratio is 8.4. Triassic Hamchang granite of the Ogcheon terrain is composed of high-alkali and high-REE group, averaged as 508 ppm REE+Y, with L/HREE=19.0, and low-alkali and low-REE group averaged as 127 ppm REE+Y with L/HREE=23. On the contrary, the early Jurassic Hapcheon syenite at southeastern margin of the Yeongnam massif is low in REE+Y (171-217 ppm). The Paleogene Gigye granite in the Gyeongsang basin, which can be a split-off part along the Yangsan fault from the REE-rich alkaline Namsan body, contains 200-300 ppm REE+Y.

Soil samples were collected from the weathered crust of these granitoids and compared with those of unweathered granitoid values.The soil values are generally lower than those of the unweathered granites in the Daegang granite (414 ppm REE+Y in rock vs. 240 ppm REE+Y in soil) and Gigye granite (342 vs. 243 ppm REE+Y), indicating most of the REE leached out during the weathering. The loss-and-gain is unclear on the Hamchang granite and Hapcheon syenite. No clear enrichment of REE during weathering has been so far observed on the granitic bodies in South Korea.

Keywords: South Korea, Mesozoic, granitoids, A-type, weathered crust, REE

1. Introduction

Rare earth element (REE) mineral resources have become important in the recent so-called high-technology industry. Finding of new REE resources, heavy REE in particular, will be a great necessity in the coming years (Ishihara and Murakami, 2005). Recent supply of REE resources in the world heavily rely on the Bayun Obo mine, Inner Mongolia, China, because of stopping of mining operation at the Mountain Pass carbonatite deposits in California, U.S.A.

Major REE-bearing ore deposits occur associated with carbonatite, alkaline granites, hydrothermal deposits of granitic affinities. There are unique ore deposits of ion-absorption type in southern China (Wu *et al.*, 1990). In these REE deposits, rare earth components are absorbed in the weathered clay minerals in granitic crusts with the enrichment factors up to 2-3 (Ishihara and Murakami, 2005). REE resources of this kind have been rarely studied at outside of the southern China but in Thailand (Kamitani and Hirano, 1994).

In this report, a reconnaissance study was made in South Korea, visiting four alkaline granitic bodies (Fig.1) where high REE contents have been known sporadically. Samples were taken from fresh granites and nearby weathering crust. Decomposed granite is divided downwards into (i) surface soil with organic matter (A horizon), (ii) completely weathered next horizon (B horizon), and (iii) weakly weathered horizon below it (C horizon). The best enrichment of REE is generally obtained from the B horizon (Huang *et al.*, 1989; Wu *et al*, 1990). Therefore, soil from the B horizon was collected generally, and its REE composition was compared with that of the nearby fresh granites. During this field work, the A horizon was found poorly developed in South Korea.

Localities of the analyzed samples are listed in Table 1, and the analytical results are given in Tables 2 to 4.

2. General Geology

South Korea is divided into four tectonic provinces with the northeasterly trends; namely, from north to south, Gyeonggi massif, Ogcheon belt, Yeongnam

[1]National Institute of Advanced Industrial Science and Technology (AIST), Central 7, 1-1-1 Higashi, Tsukuba 305-8567, Japan.
[2] Institute for Geo-Resources and Environment, GSJ, Central 7, 1-1-1 Higashi, Tsukuba 305-8567, Japan.
[3] Gyeongsang National University, 900 Gajwa-dong, Jinju, 660-701 South Korea.

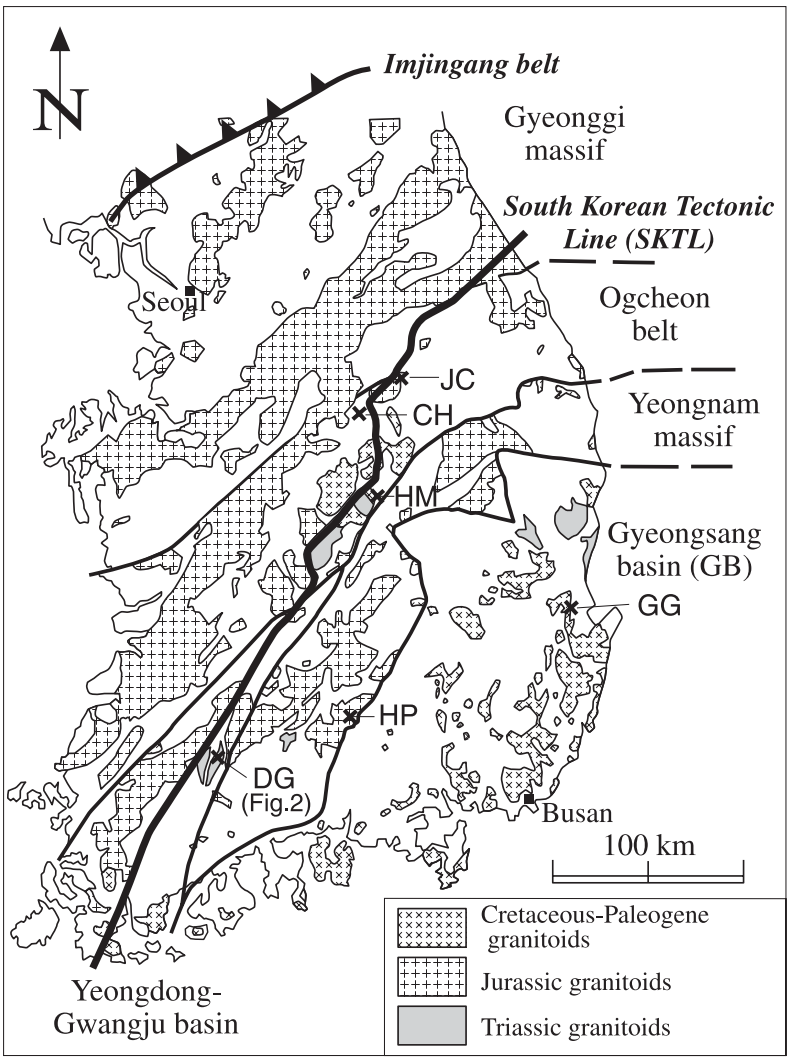

Fig. 1 Tectonic division and studied areas in South Korea. **1**. Daegang granite, **2**. Hamchang granite, **3**. Gigye granite, **4**. Hapcheon syenite. CH, Chungju REE magnetite deposit; JC, Jecheon granite (Ishihara *et al*., 2005).

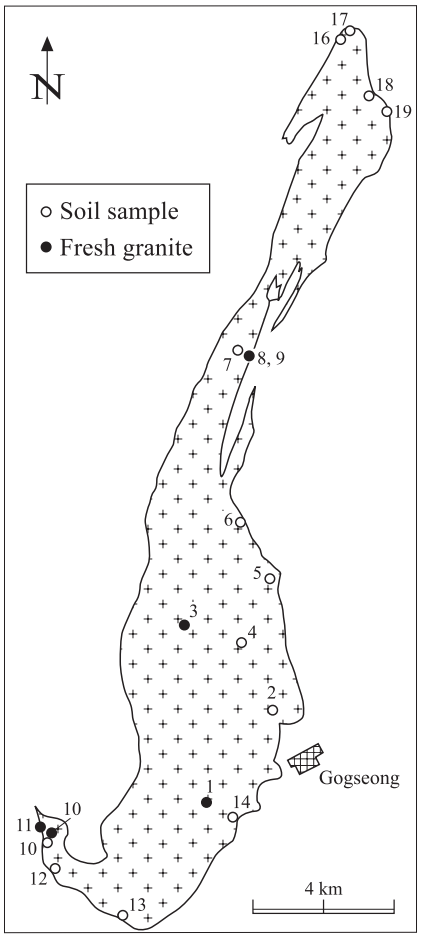

Fig. 2 Outline and sample locality of the Daegang granite.

massif and Gyeongsang basin (Fig. 1). The Gyeonggi massif and Yeongnam massif are Precambrian metamorphic terrains, but the Ogcheon belt is composed of Paleozoic sedimentary and metamorphic rocks. These terrains are intruded by Mesozoic granitoids. The southeastern corner is Cretaceous to Paleogene sedimentary-volcanic basin intruded by coeval gabbroids and granitoids.

The granitoids are mostly Jurassic and Cretaceous but locally Triassic and Paleogene in age. They are generally composed of Triassic deep-seated ilmenite-series stock, Jurassic deep-seated ilmenite-series batholiths and the Cretaceous-Paleogene magnetite-series volcano-plutonic complexes (Jwa, 2004; Jin *et al*., 2001). Almost all the granitoids belong to calc-alkaline series, but associated with small alkaline-series bodies, which can be called A type (Koh *et al*., 1996; Kim *et al*., 1998).

2.1 Daegang granite

The Daegang granite occurs along the tectonic boundary between the Yeongnam massif and the Ogcheon belt, and forms a narrow elongated body in NNE-SSW direction (Fig. 2). The basement rocks are mainly composed of the Precambrian metamorphic complex with intercalation of amphibole schist and crystalline limestone (Kim *et al*., 1990; Kim and Kim, 1990). Age-unknown metasedimentary rocks cover unconformably the basement. The Daegang granite intruded both the basement and the metasedimentary rocks during Triassic time. Radiometric ages for the granite were reported as 228 ±5 Ma by Rb-Sr whole-rock method (Choo and Kim, 1986), and 212±2 Ma by U-Pb zircon dating (Turek and Kim, 1995).

The Daegang granite is coarse-grained gray granite usually foliated in a north-south direction. The foliation is parallel to the elongation of the plutonic body,

Table 1 Locality, rock description and magnetic susceptibility of the analyzed fresh samples in South Korea.

Numbers	Rock types and magnetic susceptibility (MS)
Daegang granite, Gokseong-gun, Jeollanam-do	
R1	Coarse, biotite granite, foliated; MS=6.10 x 10^{-3}SI
R3	Coarse, biotite granite, foliated; MS=1.60 x 10^{-3}SI
R3e	Fine, enclave in the above granite; MS=0.16 x 10^{-3}SI
R3a	Medium, dike-like aplite; MS=6.12 x 10^{-3}SI
R8	Coarse, red biotite granite, foliated strongly; MS=0.12 x 10^{-3}SI
R9	100 m west of R8. Medium, biotite granite, foliated; MS=0.10 x10^{-3}SI
R10	Medium, biotite granite, strongly foliated in parts; MS=0.11 x 10^{-3}SI
R11a	Fine, leucogranite, foliated and pegmatitic; MS=0.06 x10^{-3}SI
Hamchang granite, Sangju-si, Gyeongsangbuk-do	
R21	Anryeonji dam site. Coarse, biotite granite; MS=0.14 x10^{-3}SI
R22	ditto. Fine granodiorite, pink Kf; MS=0.14 x10^{-3}SI
R22m	ditto. Medium, granodiorite, foliated weakly; MS=0.10 x10^{-3}SI
R28	ditto. Coarse, biotite granite, pink Kf; MS=0.12 x10^{-3}SI
R29	ditto. Coarse, biotite granite, pink Kf; MS=0.18 x10^{-3}SI
Gigye granite, Pohang-si, Gyeongsangbuk-do	
R30	Gigye quarry. Fine biotite granite, micro-pegmatitic; MS=0.95 x 10^{-3}SI
R31	400 m south of R30. Fine biotite granite, porphyritic; MS=0.26 x10^{-3}SI
Hapcheon syenite, Hapcheon-gun, Gyeosangnam-do	
R33	Daepyong. Medium, gray monzonite; MS= 40.2 x10^{-3}SI
R34	5 km east of R33. Coarse, biotite syenite; MS=17.1 x10^{-3}SI
R35	Daepyong, water fall; fine reddish microgranite sheet (20 cm wide); MS=2.9 x10^{-3}SI

which is strongly sheared locally. The foliation is considered caused by tectonic stress during the intrusion of the original magmas. This granite essentially belongs to the ilmenite-series of Ishihara (1977), because the magnetic susceptibility is generally lower than 0.2 x10^{-3} SI unit (Table 1), except for the R1 of 6.1x10^{-3} SI, which exceeds the upper limit of ilmenite series of 3.0 x10^{-3} SI.

The Daegang granite is represented by one feldspar hypersolvus granite containing small amounts of mafic silicates, and is classified to an alkali feldspar granite in the IUGS discrimination (Kim *et al*., 1998). The mafic silicates are small amounts of Fe-rich annite accompanied with alkaline amphibole of riebeckite. The granite has very similar mineralogical and geochemical characteristics to the A-type granites (Kim *et al*., 1998).

2.2 Hamchang granite

The Hamchang granite occurs in the middle part of the Ogcheon belt and forms a stock. The granite intruded the Precambrian metamorphic rocks, age-unknown metasedimentary rocks and the Paleozoic sedimentary rocks, but it was unconformably overlain by the Mesozoic sedimentary rocks (Choi *et al*., 1993).

Choe and Jwa (1998) considered the Hamchang granite as a member of the Jeomchon granite complex, which is composed of the Paleozoic-Triassic ilmenite-series hornblende-biotite granodiorite and deformed biotite granite, and younger intermediate-series biotite granite and magnetite-series granite porphyry. Since the deformed structure observed in the granitoids seems likely to have been caused by Jurassic Kumiri shear deformation (Hwang *et al*., 1992), the emplacement of the granitoids must have been earlier than the Jurassic shear event.

The Jeomchon granite has U-Pb sphene ages of 224±3 Ma and 225±8 Ma (Sagong *et al*., 2005), implying it is Triassic in age. The Hamchang granite and associated granite porphyry, however, are considered younger. These rocks are biotite granites in modal composition having the modal feldspar ratio of monzogranite and syenogranite, and in part alkali granite (Choe and Jwa, 1998).

Measurement of magnetic susceptibility indicates low values, below 0.2 x10^{-3} SI, which are equivalent to those of the ilmenite series.

2.3 Gigye granite

The Gigye granite occurs as a small stock in the middle part of the sedimentary-volcanic Gyeongsang basin, comprising of non-marine sedimentary and andesitic to rhyolitic volcaniclastic rocks. The Gigye granite intruded the Cretaceous sedimentary strata and may be a split-off part of the Namsan granite, ca. 20 km north, by right lateral strike-slip faulting (Hwang, 2004). The intrusion age of the Namsan granite is 48±2 Ma in laser ablation ICP-MS U-Pb zircon dating (Y.J. Jwa, unpublished data), thus Paleogene.

Both the Gigye granite and the Namsan granite show very similar petrographic and geochemical characteristics (Lee *et al*., 1995; Koh *et al*., 1996; Hwang, 2004). They are mainly composed of perthite, quartz, alkaline amphibole (riebeckite and arfvedsonite), biotite (annite), and opaque minerals. Measurement of the magnetic susceptibility on the sampling sites indicates low values as 0.2 to 3.5x10^{-3} SI unit, corresponding to ilmenite series. Chemical compositions of the granites suggest that they are strongly of the A-type granites (Koh *et al*., 1996).

2.4 Hapcheon syenite

The Hapcheon syenite occurs at the southeastern margin of the exposed Yeongnam massif, and is locally covered by the Cretaceous sediments of the western Geongsang basin. This body belongs to a complex of syenite-diorite-gabbro association, and can be interpreted as a later intrusive rock than the other rock types. It is medium to coarse-grained rock and mainly

Table 2 Polarized XRF analyses of the studied granites.

Plutons	Daegang Granite								Hamchang Granite				
Sample nos.	R1	R3	R3e	R3a	R8	R9	R10	R11a	R21	R22	R22m	R28	R29
SiO_2 wt%	74.76	75.80	70.75	76.68	74.31	73.96	74.81	75.12	71.43	71.21	68.65	70.14	71.23
TiO_2	0.22	0.11	0.25	0.09	0.18	0.19	0.19	0.03	0.20	0.28	0.35	0.27	0.32
Al_2O_3	12.32	12.39	14.30	11.99	12.55	12.73	12.90	13.96	14.21	13.85	15.49	14.61	13.74
Fe_2O_3	2.37	1.26	2.70	1.31	2.33	2.36	1.52	0.51	2.23	2.07	2.85	2.79	3.19
MnO	0.03	0.02	0.04	0.02	0.04	0.04	0.02	0.01	0.04	0.03	0.04	0.04	0.05
MgO	0.14	0.07	0.20	0.04	0.08	0.06	0.17	0.07	0.11	1.04	1.21	0.25	0.24
CaO	0.46	0.47	0.89	0.40	0.52	0.58	0.60	0.74	1.01	2.15	2.61	1.06	1.09
Na_2O	3.97	4.13	5.17	3.93	4.24	4.21	3.95	4.42	3.59	3.65	4.23	3.64	3.57
K_2O	4.67	4.96	4.70	4.73	4.96	5.19	4.91	4.57	6.00	3.95	3.52	6.17	5.55
P_2O_5	<0.01	<0.01	0.02	<0.01	<0.01	<0.01	<0.01	<0.01	<0.01	0.05	0.08	0.03	0.05
H_2O^+	0.51	0.33	0.46	0.30	0.33	0.31	0.61	0.33	0.54	0.73	0.68	0.62	0.61
H_2O^-	0.14	0.15	0.26	0.13	0.12	0.13	0.17	0.15	0.08	0.19	0.13	0.25	0.16
S	0.02	0.02	0.02	0.02	0.01	0.02	0.02	0.01	0.01	0.01	0.01	0.01	0.01
CO_2	0.17	0.11	0.07	0.10	0.04	0.07	0.57	0.06	0.62	0.61	0.08	0.41	0.20
F	0.18	0.11	0.35	0.13	0.11	0.15	0.11	0.02	0.06	0.07	0.06	0.05	0.06
Total	99.96	99.93	100.18	99.87	99.82	100.00	100.55	100.00	100.13	99.89	99.99	100.34	100.07
Rb ppm	209	239	289	235	171	154	191	183	156	101	86	153	171
Sr	29	25	26	14	11	13	70	57	77	459	545	88	98
Ba	121	109	132	35	66	66	220	170	295	1180	1020	411	426
Zr	476	184	336	53	464	457	159	22	268	71	114	326	413
Hf	14.5	7.3	9.5	4.7	11.4	10.5	6.2	1.6	6.1	1.0	2.2	6.6	10.9
Nb	26	15.9	21	20	19.6	17.7	9.4	6.7	11.6	2.4	3.6	12.3	14.8
Ta	3.6	3.8	2.7	3.8	2.3	1.9	2.8	3.5	2.8	1.2	1.1	2.2	3.0
Y	76	52	61	56	68	50	43	16	25	4	4	27	36
La	111	74	145	26	137	114	92	9	118	24	30	148	137
Ce	206	131	256	55	218	209	122	15	203	40	51	257	240
V	9	<2	2	3	<2	<2	<2	3	<3	23	30	<4	<4
Cr	12	12	10	6	9	19	9	24	11	36	36	11	13
Co	<5	<5	<5	<5	<5	<5	<5	<2	<5	<5	<5	<5	<5
Ni	4	3	1	2	3	3	3	3	2	10	10	2	3
Cu	0.4	6.3	0.9	1.2	<0.6	1.1	1.0	0.7	0.3	1.9	1.5	0.4	2.4
Zn	107	61	112	62	94	86	43	25	43	38	41	51	62
Pb	30	35	29	39	28	14	29	38	27	20	21	26	28
Ga	23.5	22.7	24.0	23.0	23.0	22.9	17.9	16.9	19.4	15.3	16.8	19.1	19.4
Ge	1.1	1.2	1.5	1.3	1.2	1.1	0.9	1.4	1.0	0.9	1.0	1.0	1.1
Se	0.4	0.3	0.3	0.3	0.2	0.2	0.3	0.2	0.2	0.3	0.2	<0.1	1.0
Mo	2.0	1.5	0.8	1.5	<0.2	2.7	<0.2	<0.2	0.3	<0.2	<0.2	1.5	3.7
W	<2	<1	<2	<1	<2	<1	<1	<1	<1	<1	<1	<1	<1
Sn	6.1	4.7	19.3	7.2	3.8	3.2	5.4	5.5	2.0	0.8	0.9	2.0	2.8
Cs	3.0	8.3	14.7	5.2	7.4	7.2	4.0	5.5	1.4	4.6	2.9	4.3	1.9
Tl	2.9	2.2	2.7	2.2	1.4	1.4	1.5	1.7	1.5	0.9	0.8	1.4	3.9
Bi	1.0	0.7	0.6	0.4	0.6	0.4	0.3	0.6	<0.3	<0.3	0.5	0.3	1.3
Th	28	24	42	33	23	22	32	3.7	28	12.4	9.3	26	32
U	3.3	5.6	5.2	4.1	3.4	1.9	4.4	1.4	2.2	<0.5	0.4	<0.5	3.3
CNK/A	0.99	0.95	0.94	0.97	0.94	0.94	1.00	1.03	1.00	0.98	1.00	1.00	0.99
10000xGa/A	3.61	3.46	3.17	3.63	3.46	3.40	2.62	2.29	2.58	2.09	2.05	2.47	2.67
Rb/Sr	7.21	9.56	11.12	16.79	15.55	11.85	2.73	3.21	2.03	0.22	0.16	1.74	1.74
Sr/Y	0.38	0.48	0.43	0.25	0.16	0.26	1.63	3.56	3.08	114.75	136.25	3.26	2.72

Analyst: B. W. Chappell, GEOMOC, Sydney. F analyzed by ISE method (Actlabs. Ltd)

comprises microcline, perthite, amphibole and subordinate amount of quartz. Diorite, which was intruded by the syenite, has much more amount of mafic minerals (20-30%) and shows a foliated texture. They are classified as the magnetite series, based on measurement of the magnetic susceptibility ($15\text{-}30 \times 10^{-3}$ SI). Though the radiometric ages of syenite and diorite are unknown, they are assumed to be early Jurassic on the basis of regional igneous activity around the area where the rocks are distributed (Kim and Turek, 1996).

3. Petrography and Chemical Compositions

Localities, rock types and magnetic susceptibility as measured by field apparatus (Kappameter KT-5) of the analyzed samples are listed in Table 1. The analytical results are given in Tables 2 and 3.

The Daegang granite belongs to the ilmenite series, and is rich in both Na_2O+K_2O and K_2O, and plotted in the high-K calc-alkaline series (Fig. 3). It has very low contents of CaO as 0.4-0.9%, and Ba content (35-220

Table 2 (continued).

Plutons	Gigye Granite		Hapcheon Syenite		
Sample nos.	R30	R31	R33	R34	R35
SiO_2 wt.%	76.10	76.37	62.45	62.79	73.02
TiO_2	0.10	0.11	0.67	0.48	0.24
Al_2O_3	11.81	11.59	16.84	18.19	13.95
Fe_2O_3	2.20	1.94	5.25	3.25	1.46
MnO	0.05	0.04	0.14	0.07	0.03
MgO	0.06	0.09	0.57	0.52	0.32
CaO	<0.01	0.30	1.21	1.80	0.65
Na_2O	4.56	4.68	6.98	6.85	4.13
K_2O	4.32	4.34	5.24	4.96	5.43
P_2O_5	<0.01	<0.01	0.16	0.17	0.02
H_2O^+	0.38	0.21	0.33	0.34	0.47
H_2O^-	0.19	0.13	0.19	0.17	0.18
S	<0.01	<0.01	<0.01	<0.01	<0.01
CO_2	0.07	0.07	0.14	0.17	0.12
F	0.05	0.17	0.04	0.04	0.03
Total	99.89	100.04	100.21	99.80	100.05
Rb ppm	167	144	67	85	179
Sr	9.0	17	91	345	157
Ba	69	99	615	960	750
Zr	514	396	106	235	223
Hf	17.0	14.2	2.7	5.7	5.7
Nb	39	28	1.1	2.6	6.4
Ta	5.2	4.5	1.2	<2	1.5
Y	93	97	28	19	17
La	56	77	30	23	43
Ce	49	110	70	48	63
V	<2	5	<5	8	12
Cr	12	11	14	9	9
Co	6	<5	<5	7	<5
Ni	4	4	1	3	4
Cu	0.6	1.5	4.1	2.7	3.1
Zn	209	100	118	55	26
Pb	26	21	10	23	17
Ga	23.0	21.4	26.5	21.1	14.5
Ge	1.9	1.5	1.6	1.0	1.0
Se	0.4	0.3	0.3	0.9	0.6
Mo	2.6	2.0	2.0	4.3	3.3
W	<2	<2	<2	<1	<1
Sn	11.9	7.5	1.5	1.5	1.3
Cs	2.3	3.2	<1.5	2.5	8.5
Tl	2.8	2.4	1.2	3.5	2.7
Bi	1.0	0.9	0.4	1.7	1.4
Th	24	18.9	0.6	6.0	27
U	8.0	4.9	0.6	5.3	8.5
CNK/A	0.97	0.90	0.87	0.91	1.01
10000xGa/A	3.68	3.49	2.97	2.19	1.96
Rb/Sr	18.56	8.47	0.74	0.25	1.14
Sr/Y	0.10	0.18	3.25	18.16	9.24

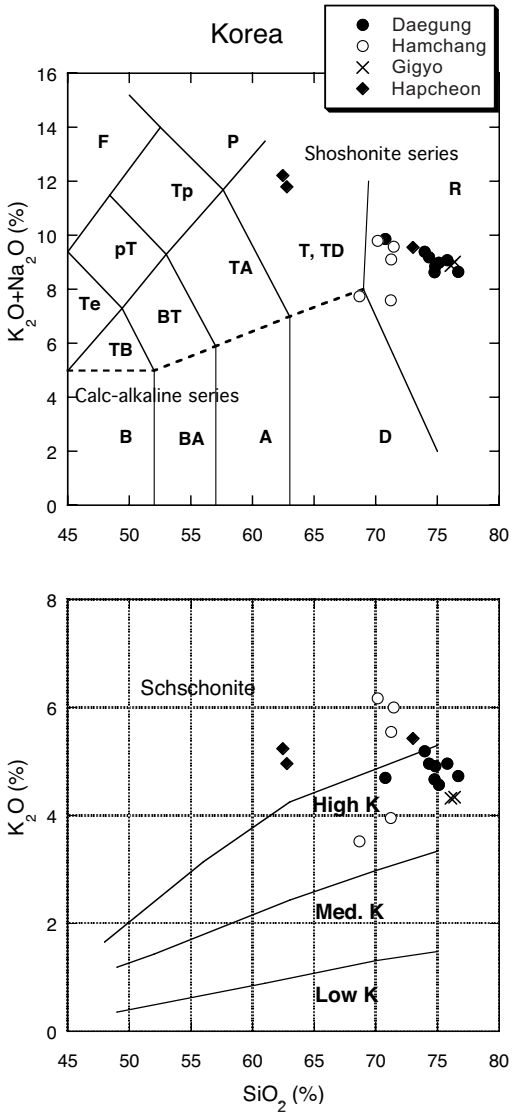

Fig. 3 Total alkalis vs. silica and potassium vs. silica contents of the studied granites. The classification based upon Le Maitre *et al.* (1989). Abbreviation: D, dacite, R, rhyolite; T, trachyte (qz<20%), TD, trachydacite (qz>20%).

ppm) and Sr content (11-70 ppm) are also low, reflecting one feldspar characteristic of the granite. The CNK/A ratio is below 1, which is meta-aluminous, except for a minor phase of the leucogranite (R11). The Ga contents (18-24 ppm) are not high, but Ga/Al x 10,000 value is higher than 2.6 (Fig. 4), thus plotted in the A-type field (Wahlen *et al.*, 1982), because of relatively low Al_2O_3 contents.

The Hamchang granite also belongs to ilmenite series (Table 1). The analyzed samples are divided into two groups on the alkali contents; high-alkali group is plotted in the shoshonite field, but the low one in the high-K calc-alkaline field (Fig. 3). Alumina saturation of the two groups is almost the same, CNK/A ratio around 1, but the low alkali group has very high contents of Sr (459-545 ppm) and Ba (1,020-1,180 ppm), and low contents of Y (4 ppm). The obtained high Sr/Y ratios (115-136, Table 2) are suggestive for adakitic nature coexisting with shoshonite-series granites. The high Sr/Y granites have been known in the Jecheon pluton, though the age is Triassic-Jurassic, to 50 km north of this body (Ishihara *et al.*, 2005).

The Gigye granite of the studied two samples belong to ilmenite series and high-K series (Fig. 3). CaO

Table 3 ICP-ICP/MS analyses of the studied granites.

	Daegang granite								Hamchang granite				
Element:	R1	R3	R3e	R3a	R8	R9	R10	R11a	R21	R22	R22m	R28	R29
Rb	204	234	299	232	172	153	194	196	167	104	94	162	185
Sr	27	24	27	15	13	15	68	58	78	423	515	87	94
Ba	124	106	135	35	63	64	230	190	323	1230	1120	438	480
Cs	3.7	4.7	12.9	3.8	4.0	6.1	2.1	5.4	1.7	2.9	2.6	2.2	2.7
Ga	27	25	28	26	27	26	21	20	23	18	20	24	25
Ge	1.7	1.5	1.9	1.5	1.6	1.4	1.3	1.7	1.3	0.9	1	1.3	1.6
La	94.9	57.2	121	18.7	115	90.9	74.3	7.85	102	34.4	34.5	124	130
Ce	183	110	227	44.7	192	175	106	14.9	186	58.7	58.2	229	237
Pr	21.5	12.5	25.1	6.07	24.4	20.5	14.5	1.86	21.2	6.24	6.08	26.4	27.7
Nd	72.9	41.4	76.1	27.1	79.4	66.9	43.7	7.66	64.9	19	18.5	81.6	87
Sm	14.1	8.15	13.1	6.47	15.2	12.7	8.19	1.92	9.79	2.72	2.68	12.1	13.8
Eu	0.392	0.266	0.403	0.132	0.206	0.188	0.56	0.221	0.869	0.617	0.775	1.11	1.13
LREE	386.79	229.52	462.70	103.17	426.21	366.19	247.25	34.41	384.76	121.68	120.74	474.21	496.63
Gd	12.9	7.61	10.1	7.17	14.0	10.6	7.56	2.19	6.79	1.77	1.72	7.82	9.32
Tb	2.34	1.48	1.86	1.49	2.24	1.77	1.3	0.49	0.98	0.25	0.26	1.11	1.42
Dy	13.6	8.71	10.3	9.43	12.0	9.67	7.3	3.17	5.11	1.34	1.39	5.69	7.29
Ho	2.71	1.78	2.06	1.92	2.34	1.84	1.45	0.6	0.95	0.25	0.25	1.05	1.38
Er	8.3	5.62	6.48	6.04	7.15	5.8	4.63	1.87	2.9	0.76	0.76	3.16	4.2
Tm	1.25	0.901	1.06	0.925	1.1	0.881	0.739	0.307	0.446	0.114	0.114	0.461	0.636
Yb	7.48	5.44	6.56	5.84	6.59	5.52	4.66	1.97	2.74	0.75	0.8	2.67	3.86
Lu	1.02	0.733	0.925	0.761	0.955	0.796	0.635	0.275	0.381	0.104	0.114	0.38	0.548
HREE	49.60	32.27	39.35	33.58	46.38	36.88	28.27	10.87	20.30	5.34	5.41	22.34	28.65
Y	74.6	51.5	61.7	55.6	69.2	51.5	43.1	20.4	27.7	7.3	8.1	29.6	39.6
HREE+Y	124.20	83.77	101.05	89.18	115.58	88.38	71.37	31.27	48.00	12.64	13.51	51.94	68.25
Zr	612	250	476	73	622	642	225	30	362	106	152	434	624
Hf	14.9	7.4	12.8	3.5	13.4	13.3	6.6	1.1	8.2	2.7	3.5	9.3	13.2
Nb	28.4	19	24.9	23.5	23.9	21.5	13.3	10.6	16.5	6.3	8	16	20.4
Ta	2.03	1.7	2	2.32	1.45	1.26	1.33	1.97	1.17	0.37	0.57	0.97	1.28
Sn	4	4	17	6	3	2	4	5	1	<1	<1	1	2
W	1.1	1	1.3	1.6	0.6	0.5	1.1	<0.5	2.7	0.6	0.7	0.7	<0.5
Tl	1.5	1.69	2.17	1.66	1.1	0.99	1.32	1.27	1	0.69	0.55	0.97	1.19
Pb	30	36	30	44	24	16	32	40	28	23	20	28	31
Sb	1.2	1.6	1.2	1.5	1.3	0.9	1.4	0.9	1.2	1.7	1	1.4	1.6
Th	27.9	24.4	43.5	33.3	25.8	22.3	32.4	6.62	29.3	13.2	10.3	29.2	38.3
U	4.17	5.64	5.8	4.22	3.61	3.34	5.5	3.51	2.91	0.94	1.47	2.27	3.36
Rb/Sr	7.6	9.8	11.1	15.5	13.2	1	2.9	3.4	2.2	0.3	0.2	1.9	2
Sr/Y	0.4	0.5	0.4	0.3	0.2	0.3	1.6	2.8	2.8	58	63.6	2.9	2.4
L/HREE	7.8	7.1	11.8	3.1	9.2	9.9	8.8	3.2	18.5	22.8	22.3	21.2	17.3
REE	436.4	261.8	502.1	136.8	472.6	403.1	275.5	45.3	405.1	127.0	126.2	496.6	525.3
REE+Y	511.0	313.3	563.8	192.4	541.8	454.6	318.6	65.7	432.8	134.3	134.3	526.2	564.9

Analyses: ICP-ICP/MS by Actlabs., Ltd. The contents in ppm

is very low, so that Ba (69-99 ppm) and Sr (9-17 ppm) are low. Zr (396-514 ppm), Zn (100-209 ppm), Nb (28-39 ppm) and Y (93-97 ppm) are high. The alumina saturation index is less than unity (Fig. 4).

The Hapcheon syenite belongs to magnetite series (Table 1) and shoshonite series in the alkali-silica plots (Fig. 3) and is meta-aluminous. The sample R33 reveals a high Ga/Al x 10,000 value as 3.0, while the others are lower than 2.2 (Fig. 4).

4. REE Contents of the Granitoids

About the Daegang granite, Kim *et al.* (1998) reported REE contents on 8 samples, and revealed the total REE varying from 301 to 662 ppm with L/HREE ratio of 5.3 to 13.1 for the normal phase (n=5), and 511 to 1,082 ppm with L/HREE ratio of 10.9 to 36.0 for the contained enclaves. Thus the enclaves are enriched in REE, especially of HREE, and the bulk contents are much depend on the amount of LREE.

Table 3 (continued).

	Gigye granite		Hapcheon syenite		
Element:	R30	R31	R33	R34	R35
Rb	164	143	65	87	189
Sr	8	16	85	331	156
Ba	70	104	677	1030	792
Cs	1.5	1.5	0.5	1.4	1.7
Ga	26	25	28	24	18
Ge	2.2	2.3	1.5	1.3	1.1
La	41.3	59.3	32.6	31.9	45.2
Ce	35.3	93.6	73.5	60.3	77
Pr	12.4	15.9	10.3	7.29	7.94
Nd	42.4	57.8	39.1	27.1	24.2
Sm	11	13.2	8.04	5.41	4.01
Eu	0.289	0.375	1.77	2.59	0.676
LREE	142.69	240.18	165.31	134.59	159.03
Gd	11.9	14.2	6.88	4.51	2.76
Tb	2.34	2.73	1.08	0.74	0.49
Dy	14.2	16	5.7	3.98	2.72
Ho	3.02	3.24	1.07	0.77	0.55
Er	10.2	10.2	3.12	2.24	1.79
Tm	1.83	1.58	0.443	0.32	0.286
Yb	11.8	10	2.75	2.05	1.86
Lu	1.73	1.42	0.4	0.306	0.281
HREE	57.02	59.37	21.44	14.92	10.74
Y	88.5	95.7	29.7	21.7	17.7
HREE+Y	145.52	155.07	51.14	36.62	28.44
Zr	646	483	175	305	273
Hf	19.4	12.8	3.3	5.9	6.1
Nb	37.3	31	6	5.3	9.7
Ta	3.23	2.42	0.28	0.36	0.79
Sn	10	7	<1	<1	<1
W	1.1	4	3.1	<0.5	<0.5
Tl	1.32	0.85	0.38	0.5	0.76
Pb	29	24	11	19	12
Sb	1.4	1.6	1.5	1.3	1.3
Th	25.4	20.1	1.36	5.95	26.5
U	7.47	4.8	0.47	1.76	2.92
Rb/Sr	20.5	8.9	0.8	0.3	1.2
Sr/Y	0.1	0.2	2.9	15.3	8.8
L/HREE	2.5	4.1	7.7	9	14.8
REE	199.7	299.5	186.8	149.5	169.8
REE+Y	288.2	395.2	216.5	171.2	187.5

Our results are lower than these values. Except for the low values of aplitic granite (R3a) and leucogranite (R11a), our REE data on 5 samples vary from 262 ppm to 473 ppm with the L/HREE ratio from 7.1 to 9.9. One enclave (R3e) is also slightly higher in REE (502 ppm, L/HREE=11.8) than the normal phase (Table 3).

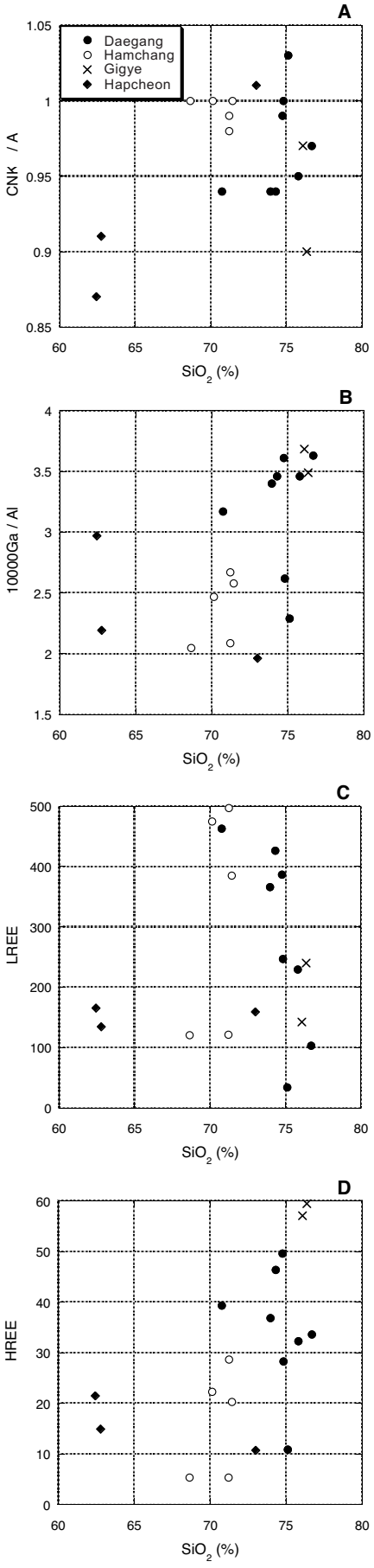

Fig. 4 CNK/A ($(CaO+Na_2O+K_2O)/Al_2O_3$, molar ratio), 10,000Ga/Al, LREE and HREE of the studied granites.

Table 4 XRF and ICP-ICP/MS analyses of the weathered soil from South Korea.

	Daegang Granite															
Element:	K1B	K2B	K4B	K5B1	K5B2	K6C	K7B	K10B	K12B	K13B	K13C	K14B	K16B	K17B	K18B	K19B
SiO_2	70.34	69.20	68.01	67.33	69.59	62.46	62.00	71.94	67.24	61.61	60.81	72.92	63.57	68.67	68.26	68.19
TiO_2	0.69	0.29	0.36	0.89	0.94	0.50	0.95	0.46	0.69	0.66	0.74	0.57	0.67	0.44	0.81	0.40
Al_2O_3	13.68	16.40	15.83	13.74	13.91	19.73	15.86	13.48	15.30	19.25	18.56	12.95	17.51	14.95	15.07	17.40
Fe_2O_3	3.90	3.48	3.62	4.57	4.70	4.14	6.42	3.00	3.70	5.26	5.23	3.35	4.89	3.25	4.22	2.61
MnO	0.07	0.02	0.01	0.04	0.04	0.04	0.12	0.02	0.06	0.04	0.06	0.03	0.06	0.03	0.05	0.02
MgO	0.94	0.30	0.31	1.09	1.13	0.75	1.52	0.44	0.65	1.21	1.80	0.47	0.88	0.57	1.21	0.66
CaO	0.18	0.04	0.03	0.08	0.09	0.26	0.91	0.13	0.07	0.62	1.80	0.06	0.06	0.15	0.43	0.54
Na_2O	1.33	0.56	1.15	0.47	0.51	0.20	1.61	1.18	0.20	0.28	1.09	0.67	0.20	0.74	0.70	1.42
K_2O	3.22	4.70	4.14	2.19	2.27	2.91	3.77	4.26	3.25	2.93	2.64	3.54	3.22	4.86	2.29	3.72
P_2O_5	0.03	0.01	0.02	0.02	0.02	0.03	0.07	0.02	0.05	0.03	0.03	0.02	0.03	0.03	0.03	0.02
Cr_2O_3	0.01	< 0.01	< 0.01	0.01	0.01	< 0.01	< 0.01	< 0.01	< 0.01	< 0.01	< 0.01	< 0.01	< 0.01	< 0.01	< 0.01	< 0.01
LOI	5.01	5.31	5.42	8.48	6.35	8.42	6.47	4.65	7.46	8.17	6.95	4.96	8.99	5.18	6.53	5.44
Total	99.40	100.31	98.90	98.91	99.56	99.44	99.70	99.58	98.67	100.06	99.71	99.54	100.08	98.87	99.60	100.42
Rb	142	191	172	114	114	105	136	154	125	149	119	132	168	257	98	132
Sr	47	18	14	46	47	74	96	40	75	71	214	28	43	42	87	180
Ba	363	154	127	388	414	840	587	253	795	563	682	241	469	373	613	966
Zr	392	825	455	343	361	162	421	557	262	223	168	525	250	313	268	152
Hf	11.8	22.6	13.6	9.5	10.1	4.8	10.5	13.7	7.2	6.4	4.8	13.5	7.4	9.4	7.9	4.5
Nb	24.6	31.2	32.1	21.5	22.2	9.2	17	19.1	16.3	13.1	9.3	25.2	16	16.7	16.8	8.6
Ta	2.17	2.42	2.63	1.67	1.72	1.27	1.34	2.01	1.76	1.45	1.51	2.23	1.65	2.28	1.57	1.38
V	62	20	33	90	90	62	75	37	61	81	85	42	71	30	71	31
Cr	40	< 20	20	60	60	< 20	40	20	40	30	40	30	40	< 20	50	< 20
Co	41	50	49	26	32	50	48	51	41	30	47	50	25	38	38	55
Ni	< 20	< 20	< 20	20	20	< 20	< 20	< 20	< 20	< 20	< 20	< 20	< 20	< 20	< 20	< 20
Cu	< 10	< 10	< 10	10	10	< 10	20	10	< 10	< 10	< 10	< 10	10	< 10	< 10	< 10
Zn	70	80	60	60	50	50	50	50	40	70	60	60	50	40	60	50
Pb	24	26	19	22	20	29	15	18	20	21	22	19	24	26	23	25
Ga	21	31	30	19	19	24	23	22	21	27	23	21	21	20	18	23
Ge	1.5	1.4	1.3	1.6	1.6	1.4	1.2	1.4	1.2	1.6	1.4	1.6	1.6	1.5	1.5	1.1
As	8	< 5	< 5	11	10	5	< 5	< 5	< 5	< 5	< 5	< 5	10	< 5	6	< 5
Mo	< 2	< 2	< 2	< 2	< 2	< 2	< 2	< 2	< 2	< 2	< 2	< 2	< 2	< 2	< 2	< 2
Sn	5	5	5	4	3	2	5	7	4	3	2	4	5	9	3	2
Sb	0.8	0.3	0.3	1.1	0.9	0.5	0.3	0.6	0.4	0.5	0.5	0.6	0.7	0.5	1	0.5
Cs	4.8	5.4	4	6.5	6.5	4.8	7.1	6.9	7.9	11.6	11.3	5	9.7	10.3	6.2	5.9
Tl	0.99	1.31	1.1	0.86	0.83	0.79	0.81	1.04	0.92	1.04	0.76	0.9	1.22	1.67	0.79	0.99
Bi	0.2	0.2	0.2	0.2	0.2	0.3	< 0.1	< 0.1	< 0.1	0.3	0.3	0.2	0.4	0.1	0.1	0.1
Th	17.7	30.4	29.9	15.7	15.1	13	15.8	16.5	13.9	20.1	17	19.1	23.3	37.8	14.4	13.8
U	3.9	5.25	4.77	3.53	3.66	5.14	2.78	3.11	2.93	3.95	3.89	3.6	4.7	7.37	3.47	2.37
La	32.1	73.0	48.0	40.0	41.6	41.5	52.5	42.3	40.5	39.2	33.0	39.7	56.7	42.7	30.8	30.9
Ce	85.9	202.0	179.0	86.5	84.6	84.6	135.0	117.0	88.2	89.4	63.6	102.0	93.1	122.0	69.0	69.6
Pr	6.8	16.0	10.6	8.3	8.9	9.0	11.0	8.3	7.7	7.5	7.5	8.4	11.2	8.4	6.6	6.0
Nd	22.8	52.4	34.8	28.0	29.3	30.4	36.1	25.8	24.4	24.3	25.7	27.9	38.2	26.7	22.5	19.8
Sm	4.26	9.71	6.99	5.02	5.29	5.50	6.32	4.51	3.99	3.98	4.43	5.19	6.22	4.64	4.04	3.07
Eu	0.65	0.38	0.42	0.99	1.04	1.11	1.10	0.45	0.89	0.97	1.23	0.56	0.96	0.53	0.84	0.67
LREE	152.5	353.5	279.8	168.8	170.7	172.1	242.0	198.4	165.6	165.4	135.4	183.8	206.4	205.0	133.7	130.0
Gd	4.59	10.00	7.19	4.26	4.69	4.53	4.82	3.93	3.37	2.99	2.86	4.36	4.74	3.49	3.07	1.77
Tb	0.92	1.85	1.50	0.79	0.85	0.72	0.93	0.84	0.55	0.54	0.47	0.97	0.95	0.68	0.54	0.26
Dy	6.00	11.10	8.77	4.38	4.80	3.53	5.03	4.92	3.17	3.07	2.64	5.93	5.42	4.12	3.24	1.27
Ho	1.28	2.35	1.80	0.87	0.95	0.64	1.03	1.03	0.65	0.60	0.50	1.23	1.02	0.87	0.68	0.22
Er	4.26	7.86	6.17	2.92	3.15	1.96	3.37	3.45	2.08	1.84	1.47	4.16	1.18	2.90	2.09	0.65
Tm	0.67	1.22	1.01	0.46	0.49	0.28	0.50	0.55	0.32	0.29	0.22	0.68	0.52	0.47	0.32	0.10
Yb	4.16	7.72	5.99	2.89	3.11	1.76	3.08	3.50	2.02	1.80	1.39	4.24	3.23	2.90	2.05	0.63
Lu	0.60	1.10	0.84	0.41	0.44	0.25	0.45	0.52	0.30	0.26	0.20	0.59	0.44	0.44	0.30	0.09
HREE	22.47	43.20	33.27	16.99	18.47	13.67	19.21	18.74	12.45	11.38	9.75	22.16	17.50	15.86	12.28	4.99
Y	38.7	69.0	55.0	27.7	30.2	18.9	29.1	31.6	20.2	19.2	15.7	39.3	33.0	26.8	20.5	7.4
L/HREE	2.5	3.2	3.2	6.2	5.7	5.3	5.0	3.9	5.1	5.4	5.3	3.0	4.1	4.8	4.1	10.6
REE	152.5	396.7	313.1	185.8	189.2	185.8	261.2	217.1	178.1	176.8	145.2	206.0	223.9	220.9	146.0	135.0
REE+Y	191.2	465.7	368.1	213.5	219.4	204.7	290.3	248.7	198.3	196.0	160.9	245.3	256.9	247.7	166.5	142.4

Analvst: Actlabs, Ltd. B and C attached to the sample numbers implving the soil from B horizon and C horizon.

The REE pattern of the granite (Fig. 5) indicates that the R11 leucogranite has the least values on most of the elements except for Eu, although it is partly pegmatitic. The R10 granite is depleted in LREE.

REE contents of the Hamchang granite are low (126 -127 ppm) in the low-alkali group of the R22 granodiorites, but high as 405 to 525 ppm in the high-alkali group of the other granites (Table 3). The L/HREE ratio is very high being 17 and 23 throughout the two groups of the granitoids, which is caused by high contents of Ce and La (Table 3). In the REE pattern (Fig. 6), the R22 granodiorites are depleted in all the components,

Table 4 (continued).

	Hamchang Granite									Gigye Granite			Hapcheon syenite
Element:	K20B	K21B	K23B	K25C	K26B	K27B	K27C	K28B	K29B	K30B	K30C	K32B	K33B
SiO_2	64.86	64.48	63.12	63.38	61.37	58.81	63.57	66.03	64.52	73.39	74.38	72.47	58.69
TiO_2	0.46	0.29	0.64	0.49	0.64	0.60	0.66	0.56	0.63	0.29	0.12	0.31	1.00
Al_2O_3	16.27	18.15	18.67	18.46	18.69	19.77	17.71	16.52	16.61	13.27	12.84	13.39	19.56
Fe_2O_3	4.35	3.29	5.30	4.07	4.88	4.97	4.31	4.45	4.75	3.15	2.31	3.09	5.64
MnO	0.18	0.01	0.05	0.03	0.02	0.03	0.03	0.04	0.09	0.07	0.05	0.03	0.11
MgO	0.75	0.27	0.74	0.47	0.57	0.61	0.58	0.97	0.71	0.31	0.12	0.26	0.48
CaO	0.21	0.13	0.19	0.05	0.32	0.09	0.21	0.27	0.37	0.07	0.05	0.05	0.31
Na_2O	1.69	2.30	1.79	0.70	2.45	0.75	0.93	0.78	1.93	1.76	2.82	2.29	3.21
K_2O	3.99	5.87	4.53	6.58	5.75	6.19	6.28	4.39	3.97	3.72	4.32	3.87	4.96
P_2O_5	0.04	0.03	0.03	0.03	0.04	0.04	0.05	0.04	0.04	0.01	< 0.01	0.01	0.04
Cr_2O_3	< 0.01	< 0.01	< 0.01	< 0.01	< 0.01	< 0.01	< 0.01	< 0.01	< 0.01	< 0.01	< 0.01	< 0.01	< 0.01
LOI	5.83	4.12	4.98	4.51	4.78	6.81	4.91	6.23	6.02	3.74	2.54	3.68	6.36
Total	98.63	98.94	100.04	98.77	99.51	98.67	99.24	100.28	99.64	99.78	99.55	99.45	100.36
Rb	118	140	134	164	140	145	145	134	145	161	171	157	105
Sr	95	68	71	66	112	84	98	56	68	17	8	14	80
Ba	589	349	668	644	730	846	833	528	560	143	86	77	677
Zr	396	448	606	427	677	504	509	373	465	812	614	293	280
Hf	10.2	12.1	15	11.4	16.5	12.1	12.6	9.8	12.2	26.7	21.8	12.3	6.7
Nb	16.4	20	24	16.7	23.6	23.6	23	16.5	24.2	54.8	41.4	46.5	16.1
Ta	1.44	1.54	1.62	1.45	1.52	1.47	1.62	1.4	1.95	4.95	4.26	4.45	1.27
V	41	17	42	18	23	29	30	52	39	20	< 5	25	25
Cr	30	< 20	30	< 20	< 20	< 20	< 20	40	30	< 20	< 20	20	< 20
Co	39	34	28	41	35	31	36	40	42	83	82	87	34
Ni	< 20	< 20	3210	< 20	< 20	< 20	< 20	< 20	< 20	< 20	< 20	< 20	< 20
Cu	< 10	< 10	20	< 10	< 10	< 10	< 10	< 10	< 10	< 10	< 10	< 10	< 10
Zn	50	< 30	70	50	60	60	50	60	80	120	130	70	40
Pb	27	22	31	30	34	34	27	24	32	39	42	14	8
Ga	21	26	25	25	26	27	23	22	24	24	26	24	24
Ge	1.2	1.1	1.6	1.2	1.3	1.5	1.3	1.3	1.6	1.8	2	1.7	1.2
As	6	< 5	6	< 5	< 5	< 5	< 5	< 5	< 5	< 5	< 5	15	< 5
Mo	3	< 2	< 2	< 2	< 2	< 2	< 2	< 2	< 2	< 2	< 2	2	< 2
Sn	3	3	3	2	3	2	2	2	4	9	10	10	1
Sb	0.4	< 0.2	1.5	0.5	0.7	0.7	0.4	0.5	0.7	0.5	0.7	0.5	0.4
Cs	3.7	1.7	5.3	2.5	2.6	2.4	2.6	4.9	5.6	4.4	2.9	5	2
Tl	0.84	0.68	1.06	1.15	1.09	1.08	0.98	0.95	1.17	1.08	1.25	1.1	0.5
Bi	0.2	0.1	0.4	< 0.1	< 0.1	0.1	< 0.1	< 0.1	< 0.1	0.5	< 0.1	0.3	< 0.1
Th	23.9	41.3	31.7	20.5	17.9	16.7	14.9	27	34.2	30.5	27.8	21.7	13
U	3.37	3.7	3.57	2.46	2.4	2.84	2.77	3.22	4	8.38	7.63	6.54	3.02
La	82.7	179.0	93.7	63.9	71.8	58.0	56.5	65.6	99.7	30.7	27.5	17.3	38.0
Ce	168.0	293.0	199.0	138.0	138.0	107.0	95.1	158.0	216.0	87.6	99.1	63.1	91.4
Pr	16.2	34.2	19.5	13.9	16.0	13.7	11.5	12.9	20.6	8.0	7.7	4.4	9.7
Nd	51.4	106.0	62.1	46.7	53.8	47.9	38.7	40.3	66.9	27.9	27.2	14.6	35.1
Sm	7.71	14.30	9.48	8.10	9.15	9.08	6.56	6.11	10.70	7.11	6.62	3.58	6.65
Eu	1.01	1.20	1.60	1.20	1.58	1.66	1.22	0.80	1.25	0.36	0.23	0.21	1.99
LREE	327.0	627.7	385.4	271.8	290.3	237.3	209.6	283.7	415.2	161.7	168.3	103.2	182.9
Gd	4.50	6.89	6.01	5.16	6.77	6.62	4.75	3.44	6.76	8.88	8.47	4.57	4.75
Tb	0.79	1.27	0.99	0.88	1.11	1.05	0.78	0.59	1.16	1.76	1.68	0.86	0.78
Dy	4.34	6.77	5.35	4.63	5.72	5.32	3.98	3.50	6.61	11.00	11.20	5.54	4.26
Ho	0.82	1.21	1.02	0.86	1.07	0.98	0.74	0.68	1.22	2.38	2.41	1.23	0.80
Er	2.55	3.73	3.22	2.48	3.18	2.96	2.27	2.12	3.71	8.57	8.67	4.51	2.51
Tm	0.39	0.55	0.51	0.36	0.47	0.44	0.34	0.33	0.58	1.52	1.49	0.85	0.39
Yb	2.46	3.51	3.14	2.31	2.87	2.73	2.09	2.08	3.56	10.30	10.10	5.92	2.65
Lu	0.35	0.49	0.48	0.33	0.40	0.40	0.30	0.30	0.51	1.56	1.49	0.90	0.43
HREE	16.19	24.42	20.71	17.00	21.59	20.50	15.25	13.04	24.11	45.97	45.51	24.37	16.56
Y	24.8	37.8	30.6	22.6	32.6	28.9	23.3	20.7	37.7	70.6	76.6	33.4	21.9
L/HREE	8.0	10.1	7.5	6.9	5.4	4.8	5.4	8.4	6.7	1.4	1.4	1.8	4.8
REE	343.2	652.1	406.1	288.8	311.9	257.8	511.6	296.7	439.3	207.7	213.8	127.6	199.5
REE+Y	368.0	689.9	436.7	311.4	344.5	286.7	534.9	317.4	477.0	278.3	290.4	161.0	221.4

but the other granitoids with similar SiO_2 contents are much higher in the REE components.

The Gigye granite could be a split-off part of the Namsan granite. The Namsan granite consists of hypersolvus alkali-feldspar granite in the northern part and subsolvus biotite granite in the southern part. The hypersolvus granite is enriched in REE, ranging from 139 to 466 ppm (Koh *et al.*, 1996). The Gigye granite of our study contains 200-300 ppm REE, not as high as the hypersolvus granite of the Namsan pluton. The L/HREE ratios range from 2.5 to 4.1, implying relatively high amounts of HREE (Table 3). The REE pattern

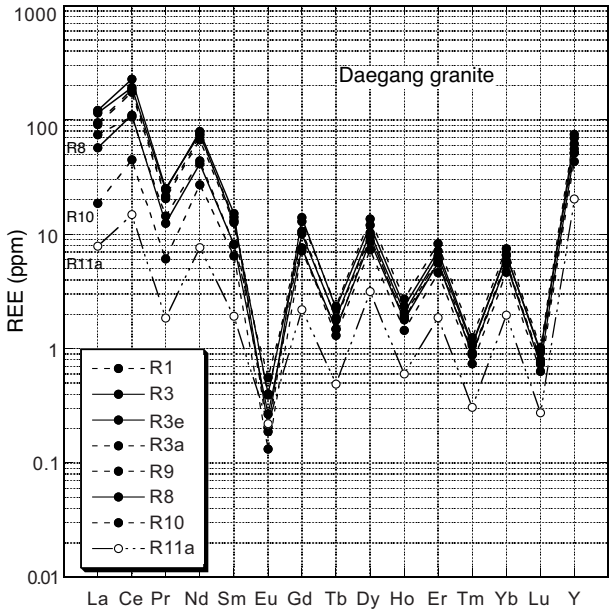

Fig. 5 REE pattern of the Daegang granite.

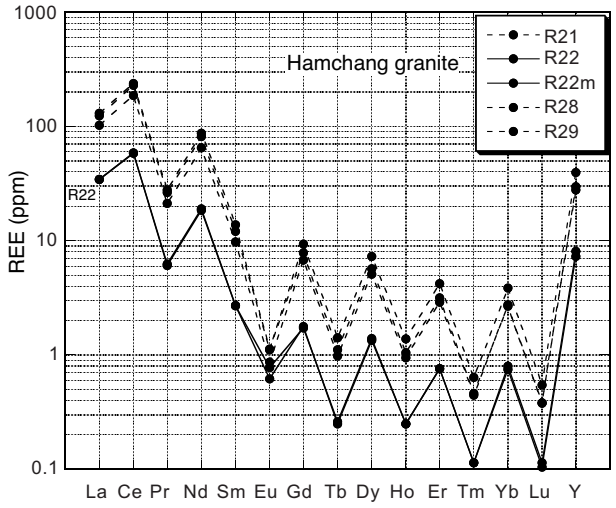

Fig. 6 REE pattern of the Hamchang granite.

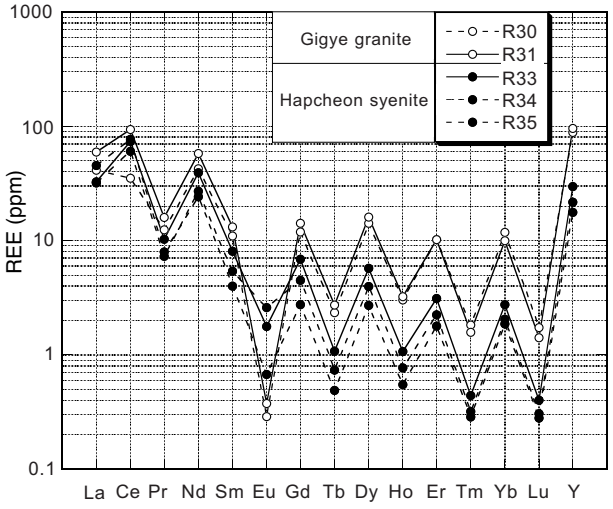

Fig. 7 REE pattern of the Gigye and Hapcheon granites.

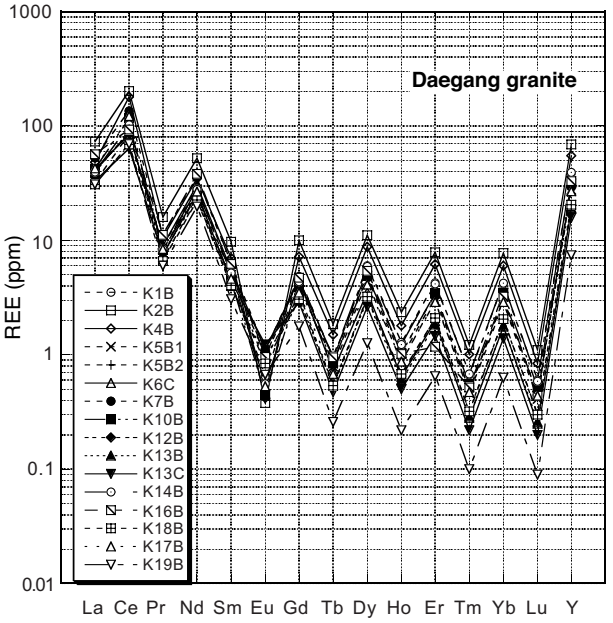

Fig. 8 REE pattern of the soil samples from the Daegang granite.

shows a strong depletion on the Eu content (Fig. 7).

The Hapcheon syenite is low in the total REE, which varies from 150 to 187 ppm. The L/HREE ratio varies from 8 to 15 (Table 3). The syenite has weak depletion of Eu, compared with the Gigye granite (Fig. 7).

5. REE during Weathering

Annual rain fall of the studied areas varies from 1,200 to 1,600 mm (KMA, 2005), which are similar to that of the southern Jiangxi Province, China, where lateritic REE deposits have been developed in the weathered crust of the Yanshanian granitoids (Wu *et al.*, 1990). Weathered crust of the studied granitic rocks in South Korea were usually developed down to 2 meters from the surface, which is mostly"B"horizon. The horizons"A"and"C"are not well developed in the studied areas. Besides, angular granitic blocks were observed at many outcrops, suggesting that debris slide modified the crust during the weathering processes.

All the soil samples were chemically analyzed and their mineral assemblages were examined by X-ray powder diffraction method. The samples examined in this study consist mainly of quartz, plagioclase and K-feldspar with small amounts of clay minerals, including kaolinite, halloysite, illite and kaolinite-montmorillonite mixed-layer mineral. Biotite has not been identified although alkalic amphibole is preserved in some

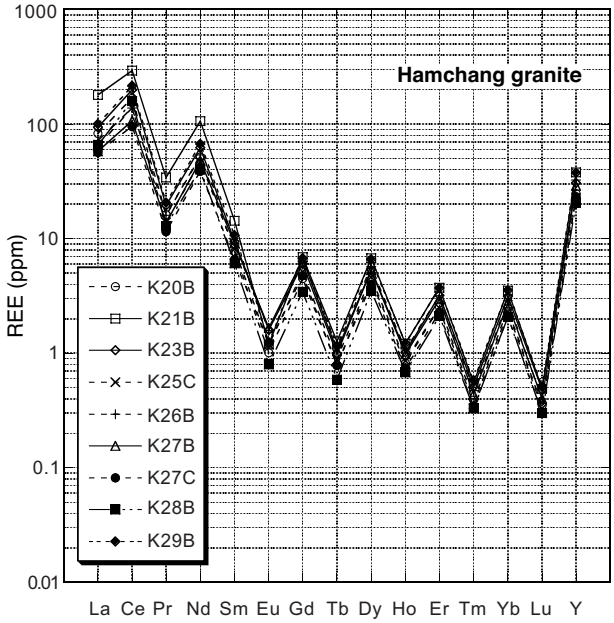

Fig. 9 REE pattern of the soil samples from the Hamchang granite.

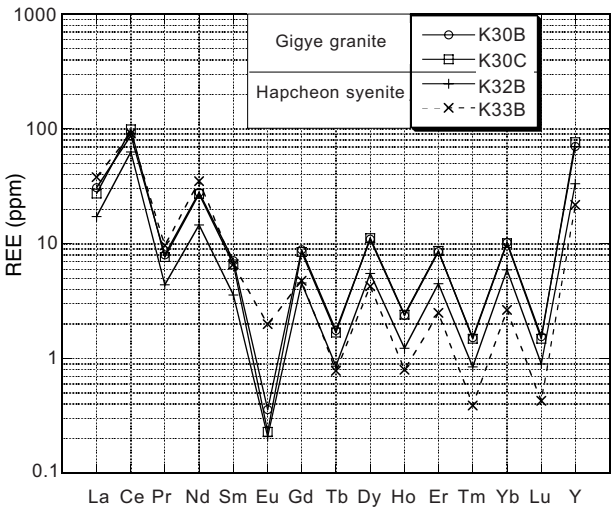

Fig. 10 REE pattern of the soil samples from the Gigye granite and Hapcheon syenite.

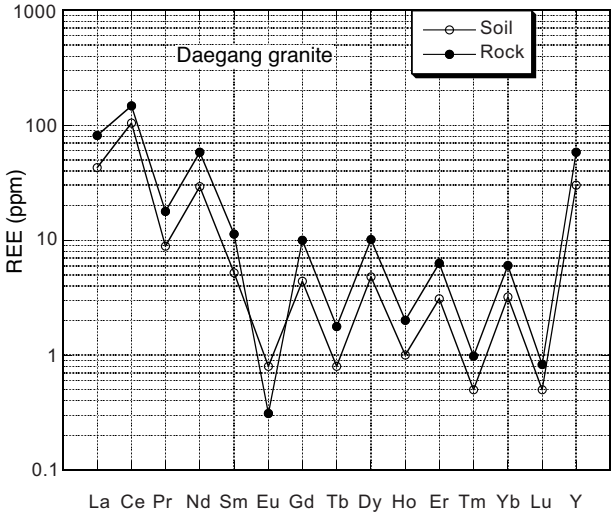

Fig. 11 REE pattern of averaged fresh rocks and soil samples of the Daegang granites.

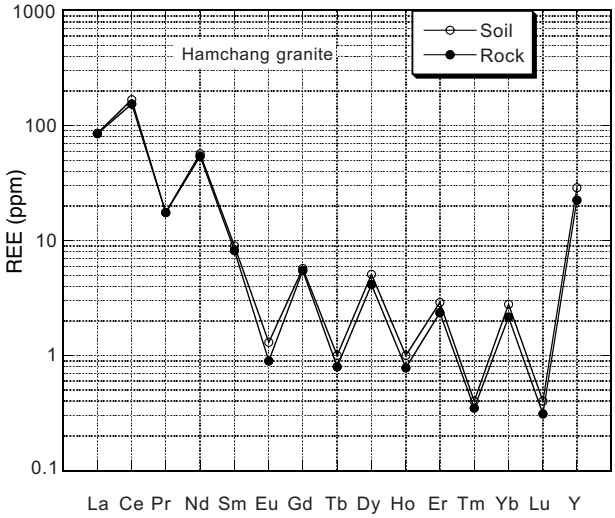

Fig. 12 REE pattern of averaged fresh rocks and soil samples of the Hamchang granites.

samples (e.g., K7B, K30B, K30C, K33B).

Feldspars are abundant in most of the samples, except for relatively clay-rich soils (K5B1, K5B2, K6C, K12B), which are characterized by high LOI (Loss On Ignition) values. B and C horizons do not show remarkable difference in their X-ray diffraction patterns. These observations suggest relatively low maturity of weathering in the studied areas. The contents of clay minerals may be approximated by LOI values, which is consistent with X-ray diffraction data. No systematic correlation has been found between the REE contents and the LOI values or assemblages of clay minerals.

Chemical compositions of studied soils are shown in Table 4. In the Daegang body, the REE+Y contents are relatively high at two points, 466 ppm (K2B) and 368 ppm (K4B), but the others are low varying from 290 ppm to 142 ppm. L/HREE ratios are generally low, as 10.6 to 2.5 (Table 4). The values are lower than those of the unweathered granites (Fig. 8), which are best shown in Figure 11. REE contents of soil samples are lower than those of the fresh granite samples, except for Eu which is enriched 2-3 times. Similar pattern is obtained on the Gigye granite (Figs. 10, 13), although number of the samples is still small. Here Eu is unchanged, and Ce is weakly enriched in the soil sample.

Average compositions of the studied rock and soil samples are given in Table 5. The rock/soil ratios of the total REE of the Daegang granite is 1.48 and that

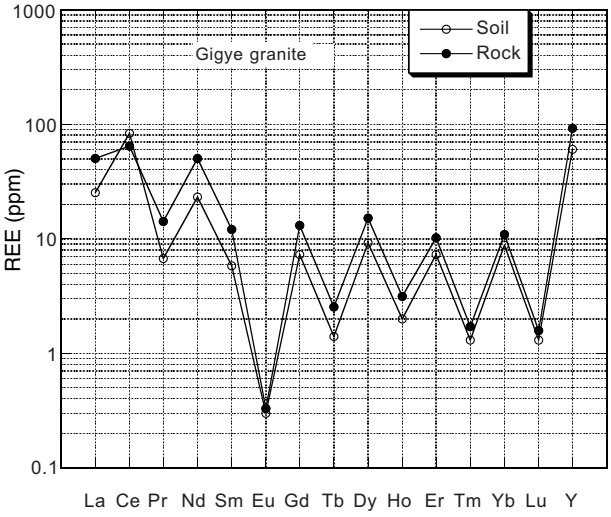

Fig. 13 REE pattern of averaged fresh rock and soil samples of the Gigye granites.

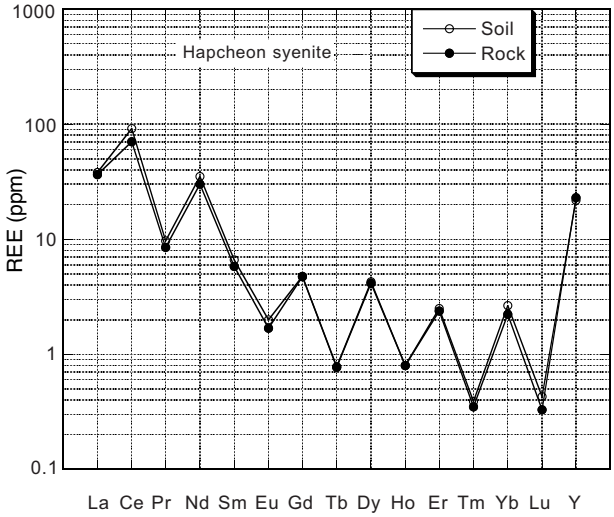

Fig. 14 REE pattern of averaged fresh rock and soil samples of the Hapcheon granites.

Table 5 Averaged REE and Y contents (ppm) of the studied fresh granites and weathered crust.

Pluton	Daegang granite		Hamchang granite		Gigye granite		Hapcheon syenite	
Saml. Nos.	1-19		20-29		30-32		33-35	
Rock/soil	Rock	Soil	Rock	Soil	Rock	Soil	Rock	Soil
La	81.7	42.8	85.0	85.7	50.3	25.2	36.6	38.0
Ce	148.0	104.5	153.8	168.0	64.5	83.3	70.3	91.4
Pr	17.8	8.9	17.5	17.6	14.2	6.7	8.5	9.7
Nd	58.2	29.3	54.2	57.1	50.1	23.2	30.1	35.1
Sm	11.3	5.2	8.2	9.0	12.1	5.8	5.8	6.7
Eu	0.3	0.8	0.9	1.3	0.3	0.3	1.7	2.0
LREE	317.3	191.5	319.6	338.7	191.5	144.5	153.0	182.8
Gd	10.0	4.4	5.5	5.7	13.1	7.3	4.7	4.8
Tb	1.8	0.8	0.8	1.0	2.5	1.4	0.8	0.8
Dy	10.1	4.8	4.2	5.1	15.1	9.2	4.1	4.3
Ho	2.0	1.0	0.8	1.0	3.1	2.0	0.8	0.8
Er	6.3	3.1	2.4	2.9	10.2	7.3	2.4	2.5
Tm	1.0	0.5	0.4	0.4	1.7	1.3	0.4	0.4
Yb	6.0	3.2	2.2	2.8	10.9	8.8	2.2	2.7
Lu	0.8	0.5	0.3	0.4	1.6	1.3	0.3	0.4
HREE	38.0	18.3	16.4	19.3	58.3	38.6	15.7	16.6
REE	355.3	209.8	336.0	358.0	249.8	183.1	168.7	199.4
Y	58.2	30.1	22.5	28.8	92.1	60.2	23.0	21.9
REE+Y	413.5	239.9	358.5	386.8	341.9	243.3	191.7	221.3
L/HREE	8.4	10.5	19.5	17.6	3.3	3.7	9.7	11.0

of the Gigye granite is 1.36. It may be concluded in these two granitic bodies that REE are generally eroded out during the weathering.

On the other two granitic bodies, the loss-and-gain during the weathering is unclear, although all the HREE looks slightly enriched during the weathering in the Hamchang granite (Figs. 9, 12, 14). The rock/soil ratios of the averaged total REE contents (Table 5) are 0.94 in the Hamchang granite and 0.85 in the Hapcheon syenite. Thus, the REEs are most enriched in the

Hapcheon syenite during weathering in the studied areas.

6. Concluding Remarks

Alkaline granites and their weathered crust were examined chemically. The granites are relatively high in trace amounts of REE+Y. The weathered crusts show no evidence of REE-enrichment but often depleted relative to the unweathered host rocks. Although ages of the studied granites are Triassic to Paleogene, the weathered crusts seem to have formed in the Quaternary by uplifting of the Korean Peninsula. This short time-span of the weathering may be the main reason of no accumulation of REE in the studied weathered crust.

Appendix: REE contents of rocks from the former Chungju REE mine

The world largest REE concentration has been known in the REE-magnetite deposits at Bayan Obo in the Inner Mongolia, China. Similar showings have been known near Chungju in the middle part of South Korea, and they are developed within the Gyemyeongsan Formation of a gneiss-schist complex (Kim *et al.*, 1994). The Chungju iron mine is one of the REE ore deposits in the Ogcheon belt, South Korea.

The REE deposit of the mine mainly contains Ce-La, Ta-Nb, Y, Y-Nd and Nd-Th group minerals (Park and Kim, 1995). More than 15 REE-bearing minerals were reported from the mine: they are allanite, fergusonite, thorite, bastnaesite, euxenite, polyclase, monazite, columbite, Nb-rutile, okanogranite, sphene, zircon, illmenite and so on. According to the characteristics of the mineral association, the REE ore deposit can be divided into four ore types: zircon-REE, allanite-REE, feldspar-REE and fluorite-REE types. The Sm-Nd isochron age of the REE deposit was reported to be 330 Ma (Park and Kim, 1995).

This mine is now abandoned and the surface is now used for crushing stone mining for construction purposes. A brief stop was made here to collect samples to estimate bulk composition of REE-bearing outcrop. The 10 hand specimens of Appendix-1 were arbitrary collected, crushed and analyzed for major (XRF) and trace elements (ICP-ICP/MS).

The analyzed samples of more or less a fist size contains more than 6,900 ppm REE+Y (K14E, Appendix-2), which are banded granitic and amphibolitic gneisses. The second highest is light gray gneiss (K14J) of >5,500 ppm. Pink felsic gneiss (K14C) is also high as >3,700 ppm. An average of these analyses, excluding K14K because it is a thin vein aplite, is as follows:

LREE >1,700 ppm, HREE> 354 ppm (LREE/HREE=4.8), and Y >362 ppm

These figures may represent an average composition of the ore deposit, and the total REE+Y content, 2,416 ppm, is one-order of magnitude lower than that of the Bayan-Obo REE-magnetite mine in China (Drew *et al.*, 1990).

References

Choe, W. H. and Jwa, Y. J. (1998) Petrochemical characteristics of the granites in the Jeomchon area. *Jour. Petrol. Soc. Korea*, **7**, 37-52 (in Korean with English abstract).

Choi, H.I., Lee, B.J., Hwang, S.G., Choi, P., Song, K.Y. and Kim, D.H. (1993) Geological Report of the Nongam Sheet (1:25,000). *Korea Inst. Energy & Resources, Seoul*, 40p (in Korean with English abstract).

Choo, S.H. and Kim, S.J. (1986) Research on Rb/Sr isotope age dating of Youngnam massif (II), Gneiss and gneissic granitoids from the southern part of Mt. Jiri. *KIGAM Research Report, KR-86-7*, 7-33 (in Korean with English abstract).

Drew, L.J., Meng, Q., and Sun, W. (1990) The Bayan Obo iron-rare earth-niobium deposits, Inner Mongolia, China. *Lithos*, **26**, 43-65.

Huang, D-H., Wu, C-Y., and Han, J-Z. (1989) REE geochemistry and mineralization characteristics of the Zudong and Guanxi granites, Jiangxi Province. *Acta Geol. Sinica*, **2**, 139-157.

Hwang, B.H. (2004) Petrology, isotope and petrogenesis of the granitic rocks in the southern Gyeongsang basin. *PhD theis, Pusan National Univeristy*, 306p (in Korean with English abstract).

Hwang, S.G., Lee, B.J. and Yoo, B.C. (1992) A phyllonite zone exposed in Sangju area: an ultramylonite caused by reaction softening. *Jour. Geol. Soc. Korea*, **28**, 410-425 (in Korean with English abstract).

Ishihara, S. (1977) The magnetite-series and ilmenite-series granitic rocks. *Mining Geol.*, **27**, 293-305.

Ishihara, S. and Murakami, H. (2005) An attractive mineral resource: heavy rare-earth - Are the ion-absorption-type deposits enough to support the modern high-technology industry? *Geology News*, no. 609, 6-18 (in Japanese).

Ishihara, S., Jin, M.S. and Terashima, S. (2005) Mo-related adakitic granitoids from non-island-arc setting: Jecheon pluton of South Korea. *Resource Geology*, **55**, 385-396.

Jin, M.S., Lee, Y. S. and Ishihara, S. (2001) Granitoids and their magnetic susceptibility in South Korea. *Resource Geol.*, **51**, 189-203.

Jwa, Y-J. (2004) Possible source rocks of Mesozoic granites in South Korea: implications for crustal evolution in NE Asia. *Trans. Royal Soc. Edinburgh: Earth Sci.*, **95**, 181-198.

Kamitani, M. and Hirano, H. ed. (1994) Study on rare-earth resources in weathered granitoids in Thailand. *Rept. Intern. Res. Develp. Coop., ITIT Project n.* 90-1-2, *Geol. Surv. Japan*, 201 p.

Kim, C.B. and Kim, Y.J. (1990) Geochronology and petrochemistry of foliated granite between Damyang and Jinan. *Jour. Korean Inst. Mining Geol.*, **23**, 233-244 (in Korean with English abstract).

Kim, C. B. and Turek, A. (1996) Advances in U-Pb zircon geochronology of Mesozoic plutonism in the southwestern part of Ryeongnam massif, Korea. *Geochem. Jour.*, **30**, 323-338.

Kim, C.B., Kim, Y.J. and Hong, S.S. (1990) Geochemical study on foliated granite in the Damyang-Jinan area. *Jour. Korean Inst. Mining Geol.*, **23**, 87-104 (in Korean with English abstract).

Kim, G.S., Park, M.E. and Enjoji, M. (1994) Banded and massive iron mineralization in Chungju mine (I): Geology and ore petrography of iron deposit. *Econ. Environ. Geol.*, **27**, 523-535.

Kim, Y-J., Cho, D-L. and Lee, C-S. (1998) Petrology, geochemistry and tectonic implication of the A-type Daegang granite in the Namwon area, southwestern part of the Korean peninsula. *Econ. Environ. Geol.*, **31**, 399-413 (in Korean with English abstract).

KMA (Korea Meterological Adminstration) (2005) Annual Climatological Report 2004. *KMA. 11-1360000-000016-10*, p. 293.

Koh, J. S., Yun, S. H. and Lee, S.W. (1996) Petrology and geochemical characteristics of A-type granite with particular reference to the Namsan Granite, Kyeonju. *Jour. Petrol. Soc. Korea*, **5**, 142-160 (in Korean with English abstract).

Le Maitre, R.W., Bateman, P., Dudek, A., Keller, J., Lameyre, J., Le Bas, M. J., Sabine, P.A., Schmid, R., Sorensen, H., Streckeisen, A., Wooddey, A.R. and Zanettin, B. (1989) A Classification of Igenous Rocks and Glossary of Terms. *Blackwell, Oxford*, 193 p.

Lee, M.J., Lee, J.I. and Lee, M.S. (1995) Mineralogy and major element geochemistry of A-type alkali granite in the Kyeongju area, Korea. *Jour. Geol. Soc. Korea*, **31**, 583-607.

Park, M.E. and Kim, G.S. (1995) Genesis of the REE ore deposits, Chungju district, Korea: Occurrence features and geochemical characteristics. *Econ. Environ. Geol.*, **28**, 599-612 (in Korean with English abstract).

Sagong, H., Kwon, S.-T. and Lee, J.-H. (2005) Mesozoic episodic magmatism in South Korea and its tectonic implication. *Tectonics*, 24, TC5002, doi:10.1029/2004TC001720.

Turek, A. and Kim, C.B. (1995) U-Pb zircon ages of Mesozoic plutons in the Damyang-Geochang area, Ryeongnam massif, Korea. *Geochem. Jour.*, **29**, 243-258.

Whalen, J. B., Currie, K.L.and Chappell, B.W. (1982) A-type granites: geochemical characteristics, discrimination and petrogenesis. *Contrib. Mineral. Petrol.*, **95**, 407-419.

Wu, C-Y., Huang, D-H. and Guo, Z-X. (1990) REE geochemistry in the weathered crust of granites, Longnan area, Jiangxi Province. *Acta Geol. Sinica*, **3**, 193-210.

Received June 26, 2006
Accepted September 21, 2006

韓国における幾つかのアルカリ花崗岩類とその風化殻のレアアース資源評価

石原舜三, 佐藤興平, 左　容周, 金　鍾善

要　旨

花崗岩風化殻へのREEの濃集を見るために，韓国の中部の花崗岩地域4箇所（平均降雨量1,300 mm/ 年）で予察的な調査を実施した．嶺南帯と沃川帯境界部に沿って伸長する三畳紀の片麻状黒雲母花崗岩（帯江岩体）はREEに富み，平均414 ppm REE+Y，LREE/HREE=4.8である．沃川帯の三畳紀咸昌（ハムチャン）花崗岩類は，アルカリとREEに富むグループ（平均359 ppm REE+Y, L/HREE=19.0）と，低いグループ（平均127 ppm REE+Y, L/HREE=23）に分けられる．他方，嶺南帯南東部の初期ジュラ紀の陜川（ハプチョン）閃長岩はREE+Y(171～217 ppm）に乏しい．慶尚盆地の杞溪（キゲ）花崗岩は南山アルカリ花崗岩の断層による片割れと言われているが，その含有量は200～300 ppm REE+Yであるに過ぎない．

完全風化帯であるB層を中心とする花崗岩風化物は，帯江岩体では花崗岩平均値が414 ppm REE+Yであるのに対し，風化土壌は240 ppm REE+Yで希土類元素が減少しており，風化課程におけるREEの溶脱が考えられる．杞溪岩体でも342 ppmから243 ppm REE+Yへ希土類元素は減少している．その他の岩体での増減は不鮮明である．韓国では花崗岩の風化課程で希土類元素の明瞭な濃集は見られない．

忠州鉄鉱床の採掘跡におけるランダム　サンプリングによると，この鉱床は平均0.2% REE+Y程度の鉱石を保有していたと推定される．

付録：漢字対照表

Daegang（帯江）granite, Gokseong-gun（谷城郡）, Jeollanam-do（全羅南道）, Hamchang（咸昌）granite, Sangju（尚州）, Gyeongsangbuk-do（慶尚北道）, Gigye（杞溪）granite, Pohang（浦項）, Hapcheon（陜川）syenite, Gyeosangnam-do（慶尚南道）

Appendix Table 1 Rock description and magnetic susceptibility (MS) of the analyzed samples from the former Chungju mine surface.

Numbers	Rock description and magnetic susceptibility(MS)
K14A: 10 x 12 cm, magnetite/ green banded gneiss. MS＞894 x10^{-3} SI	
K14B: 7x12 cm, magnetite-amphibolite gneiss. MS=156 x10^{-3} SI	
K14C: 6x7 cm, very fine, pink felsic gneiss. MS ＞53.9 x10^{-3} SI	
K14E: 8x10 cm, pink granitic vein/amphibolite(3/2)	
K14F: 7x9 cm, mudium, epidote-chlorite granodioritic gneiss. MS=1.5 x10^{-3} SI	
K14G: 9x16 cm pink biotite gneiss xenolith in pink granite. MS＞15.1 x10^{-3} SI	
K14H: 6x12 cm, pink banded gneiss. MS＞46.6 x10^{-3} SI	
K14 I 5 x 10 cm, quartz-calcite-rich gneissic band.	
K14 J: 10x10 cm, light gray skarn-gneiss. MS ＞70.2 x10^{-3} SI	
K14K: 5 cm wide veinlet of pink fine-grained aplitic granite. MS＞5.6 x10^{-3} SI.	

MS measured by Kappameter, KT-5.

Appendix Table 2 Major (XRF) and trace (ICP-ICP/MS) element compositions of rocks and ores from the Chungju mine.

Element:	K14A	K14B	K14C	K14E	K14F	K14G	K14H	K14I	K14J	K14K
SiO_2	26.48	45.97	73.39	60.33	66.09	74.39	68.92	77.42	70.10	75.37
TiO_2	0.27	3.46	0.40	1.51	0.27	0.12	0.25	0.21	0.41	0.02
Al_2O_3	1.07	14.41	8.81	14.34	16.22	12.40	9.38	2.34	8.20	13.29
Fe_2O_3	68.07	15.18	6.67	8.08	4.02	1.89	6.76	8.23	8.48	0.57
MnO	0.27	0.13	0.04	0.18	0.08	0.04	0.15	0.11	0.16	0.01
MgO	0.62	5.14	0.21	1.55	0.47	0.29	1.04	0.31	1.17	0.11
CaO	3.11	4.84	1.96	2.95	5.30	0.99	4.24	6.83	4.24	1.12
Na_2O	< 0.01	5.28	1.15	2.43	3.65	2.40	0.58	0.09	2.64	3.82
K_2O	0.02	2.73	5.52	7.03	2.18	6.14	5.98	1.15	2.78	5.01
P_2O_5	0.04	2.00	< 0.01	0.33	0.06	0.01	< 0.01	< 0.01	< 0.01	0.01
Cr_2O_3	< 0.01	< 0.01	< 0.01	0.01	< 0.01	< 0.01	< 0.01	< 0.01	< 0.01	< 0.01
LOI	0.19	0.64	1.03	1.02	1.31	0.91	1.34	2.05	0.78	0.65
Total	100.14	99.78	99.18	99.76	99.65	99.58	98.64	98.74	98.96	99.98
Rb	4	188	161	181	83	148	151	37	132	162
Sr	28	214	34	152	356	171	57	35	39	143
Ba	6	198	165	829	319	890	240	35	86	727
Zr	953	301	> 10000	829	596	1060	2800	2620	> 10000	89
Hf	25.6	7.4	311	23.2	15.8	27.9	75	70.3	291	2.7
Nb	92.7	60.8	> 1000	280	62.8	171	449	513	> 1000	32.7
Ta	7.31	4.07	143	19.4	3.96	15.9	32.4	33	120	6.01
V	11	142	< 5	76	6	< 5	< 5	< 5	< 5	< 5
Co	80	50	118	95	152	211	136	232	150	249
Cu	< 10	< 10	< 10	< 10	< 10	20	< 10	< 10	< 10	< 10
Zn	180	70	< 30	60	< 30	< 30	30	< 30	< 30	< 30
Pb	< 5	< 5	10	14	7	11	7	< 5	7	7
Ga	16	24	33	45	27	20	34	17	44	14
Ge	18.4	2	4	26.3	1.8	1.7	5.1	3.9	5.6	0.8
As	10	19	9	143	< 5	< 5	< 5	6	18	< 5
Mo	< 2	3	< 2	2	20	32	< 2	< 2	< 2	< 2
Sn	17	2	125	13	11	6	24	77	123	8
Sb	3.4	1	0.9	5.4	0.5	1.6	0.8	0.8	1.4	0.3
Cs	0.7	4	0.3	4.1	0.9	1.1	0.4	< 0.1	0.4	0.5
Tl	0.06	0.42	0.25	0.61	0.39	0.43	0.36	0.05	0.1	0.37
Bi	0.2	< 0.1	0.2	0.3	0.1	< 0.1	< 0.1	< 0.1	0.2	< 0.1
Th	7.33	5.21	257	75.7	37.7	31.3	85.5	59.8	242	14
U	4.92	2.92	71.7	4.38	2.36	5.28	33.9	20.4	65.4	0.98
La	33.1	71.3	415.0	1760.0	139.0	122.0	130.0	164.0	865.0	38.3
Ce	67.8	156.0	853.0	> 3000	242.0	233.0	313.0	354.0	1830.0	65.1
Pr	6.7	20.8	115.0	355.0	25.6	26.4	35.3	54.7	218.0	6.8
Nd	22.2	84.4	517.0	1190.0	81.9	88.6	139.0	234.0	761.0	21.6
Sm	4.6	17.1	141.0	174.0	12.7	19.2	35.9	60.9	163.0	3.8
Eu	0.5	6.3	7.6	15.3	2.3	1.4	1.7	3.1	7.7	0.7
LREE	134.9	355.9	2048.6	> 6494.3	503.5	490.6	654.9	870.7	3844.7	136.4
Gd	4.29	14.50	150.00	106.00	7.84	18.70	42.90	65.60	168.00	2.76
Tb	0.74	2.19	31.50	10.20	1.07	3.42	9.58	12.70	30.60	0.43
Dy	4.26	10.50	195.00	42.90	4.60	20.00	63.20	76.30	176.00	2.10
Ho	0.85	1.80	38.80	7.00	0.76	3.79	13.70	15.80	34.80	0.38
Er	2.68	4.76	121.00	19.50	2.10	11.20	44.00	49.50	108.00	1.11
Tm	0.46	0.64	18.60	2.60	0.29	1.66	6.59	7.56	16.80	0.16
Yb	3.34	3.72	111.00	14.90	1.83	9.89	40.10	45.90	102.00	0.99
Lu	0.57	0.52	14.60	1.86	0.32	1.32	5.48	6.13	13.50	0.14
HREE	17.19	38.63	>1680.5	204.96	18.80	69.98	225.55	279.49	649.70	8.07
Y	26.7	51.6	> 1000	202.0	21.1	112.0	377.0	464.0	> 1000	12.3
HREE+Y	43.9	90.2	>1680.5	407.0	39.9	182.0	602.6	743.5	>1649.7	20.4
L/HREE	3.1	4.0	<1.2	>16.0	12.6	2.7	1.1	1.2	< 2.3	6.7
REE+Y	178.8	446.1	>3729.1	> 6901.3	543.4	672.6	1257.5	1614.2	>5494.4	156.8

Analyist: Actlabs, Ltd. Cr and Ni, below 20 ppm